Synthesis, X-ray Structure, and Reactivity of Phosphine-Substituted Iron Carbonyl Complexes Containing σ-Alkyl−π-Allyl Ligands

Titus A. Jenny,* Vroni Huber, Liqian Ma, Jacques Raemy, and David Zeller

Institut de chimie organique, University of Fribourg, Fribourg, Switzerland

Helen Stoeckli-Evans

Institut de chimie, University of Neuchatel, Neuchatel, Switzerland

Received August 27, 2001

The synthesis, structure, and reaction chemistry of dicarbonyl phosphine and carbonyl diphosphine iron complexes with σ-alkyl−π-allyl ligands derived from ring-opened pinene systems are described. X-ray diffraction studies on three representative examples were performed and showed significant differences in the orientation of the phosphine ligands with respect to the σ-alkyl−π-allyl ligands. These differences are caused by steric interactions, as shown by the fluxional behavior of some of the complexes on the NMR time scale. The influence of the phosphine ligand is demonstrated by the reaction of these complexes with $CO/AlCl_3$ and their photolysis products in acetic acid.

Introduction

Iron carbonyl complexes having σ-alkyl−π-allyl coordinated carbon skeleton ligands are obtained in various ways: e.g., by ring-opening complexation of vinylcycloalkanes,[1] nucleophile (e.g. hydride) addition to cationic complexes containing η^5-ligands,[2] addition of reactive alkenes to diene complexes,[3] cycloadditions to diene complexes possessing an additional conjugated double bond,[4] photolysis of either diene complexes in the presence of acrylate or acrylate complexes in the presence of dienes,[5] and Lewis acid promoted CO insertion into the π-system of diene complexes.[6] Despite these numerous synthetic entries into the class of σ-alkyl−π-allyl coordinated ligands, structural information on such iron carbonyl complexes is sparse and mainly confined to examples in which the σ-coordinated carbon atom carries electron-withdrawing substituents. On the other hand, structures lacking these stabilizing electron-withdrawing substituents were frequently formulated as intermediates in reaction schemes, stressing the ephemeral nature of these compounds which tend to isomerize to the corresponding diene complexes,[7] but cases of thermally stable complexes are known.[8] We obtained a product of this type on reacting $Fe(CO)_5$ with α- or β-pinene in refluxing dioxane as a stable complex (**1**).[9] As the σ-alkyl−π-allyl ligand arises from opening of the four membered ring of the pinene skeleton, this new ligand is called *seco*-pinene. Because *seco*-pinene−$Fe(CO)_3$ (**1**) crystallizes only at temperatures below 0 °C, a crystalline phosphine derivative (**2**) was synthesized[9] by reacting complex **1** with triphenylphosphine in refluxing cyclohexane, allowing for the first time an X-ray analysis of a phosphine-substituted σ-alkyl−π-allyl iron carbonyl complex.

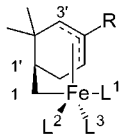

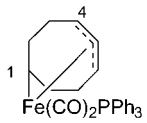

3

	R	L^1, L^2, L^3
1	CH_3	$(CO)_3$
2	CH_3	$(CO)_2PPh_3$
4	CH_3	$(CO)_2P(OMe)_3$
5	CH_3	$(CO)(P(OMe)_3)_2$
6	CH_3	$(CO)_2P(OCH_2)_3CEt$
7	H	$(CO)_3$
8	H	$PPh_3(CO)_2$

(1) Sarel, S. *Acc. Chem. Res.* **1978**, *11*, 204 and references therein.
(2) (a) Pearson, A. J.; Ong, C. W. *J. Org. Chem.* **1982**, *47*, 3780. (b) Deeming, A. J.; Ullah, S. S.; Domingos, A. J. P.; Johnson, B. F. G.; Lewis, J. *J. Chem. Soc., Dalton Trans.* **1974**, 2093. (c) Godula, K.; Donaldson, W. A. *Tetrahedron Lett.* **2001**, *42*, 153.
(3) Bond, A.; Green, M.; Lewis, B.; Lowrie, S. F. W. *J. Chem. Soc., Chem. Commun.* **1971**, 1230.
(4) (a) Paquette, L. A.; Ley, S. V.; Broadhurst, M. J.; Truesdell, D.; Fayos, J.; Clardy, J. *Tetrahedron Lett.* **1973**, 2943. (b) Green, M.; Heathcock, S.; Turney, T. W.; Mingos, D. M. P. *J. Chem. Soc., Dalton Trans.* **1977**, 204. (c) Goldschmidt, Z.; Gottlieb, H. E.; Cohen, D. *J. Organomet. Chem.* **1985**, *294*, 219. (d) Chopra, S. K.; Cunningham, D.; Kavanagh, S.; McArdle, P.; Moran, G. *J. Chem. Soc., Dalton Trans.* **1987**, 2927.
(5) (a) Grevels, F.-W.; Feldhoff, U.; Leitich, J.; Krüger, C. *J. Organomet. Chem.* **1976**, *118*, 79. (b) Grevels, F.-W.; Klotzbücher, W. *Inorg. Chem.* **1981**, *20*, 3002. (c) Goddard, R.; Grevels, F.-W.; Schrader, R. *Angew. Chem.* **1985**, *97*, 318; *Angew. Chem., Int. Ed., Engl.* **1985**, *24*, 353.
(6) (a) Heil, V.; Johnson, B. F. G.; Lewis, J.; Thompson, D. J. *J. Chem. Soc., Chem. Commun.* **1976**, 270. (b) Eilbracht, P.; Hirshfelder, A. *Adv. Met.-Org. Chem.* **1990**, *5*, 55 and references therein.
(7) Aumann, R. *J. Am. Chem. Soc.* **1974**, *96*, 2631.
(8) (a) Sarel, S.; Felzenstein, A.; Victor, R.; Yovell, J. *J. Chem. Soc., Chem. Commun.* **1974**, 1025. (b) Hayakawa, K.; Schmid, H. *Helv. Chim. Acta* **1977**, *60*, 1942.
(9) Jenny, T. A.; Ma, L. *Tetrahedron Lett.* **1991**, *32*, 6101.

10.1021/om010781s CCC: $22.00
Publication on Web 05/16/2002

Scheme 1. Synthesis of the Complexes

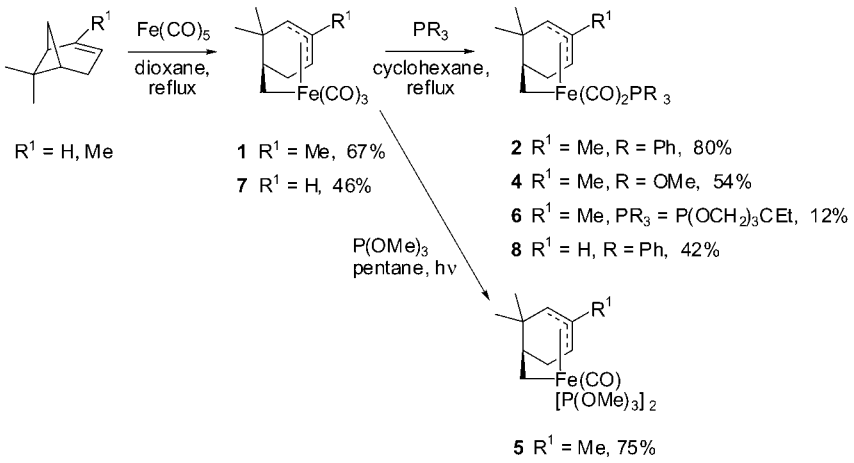

At first, it was assumed that the positioning of the phosphine ligand would be governed by electronic effects: i.e., the higher σ-donor capacity of phosphine ligands compared to CO favors a transoid arrangement with respect to the σ-bonded carbon atom of the hydrocarbon ligand. This geometry is indeed adopted in complex **3**, [(1,4,5,6-η)-5-cyclooctene-1,4-diyl]$Fe(CO)_2PPh_3$, as already inferred from its ^{1}H NMR spectrum.[2b]

It soon appeared that, in contrast to this, the triphenylphosphine ligand occupies an equatorial position in complex **2**. To understand the factors which determine the positioning of the phosphine ligand and to explain the differences in reactivity within this class of compounds, the structures of a number of related complexes were investigated.

Results and Discussion

Syntheses. The phosphine-substituted complexes (+)-**2**, (−)-**4**, **6**, and (−)-**8** were synthesized in analogy to the published procedure[2b] for complex **3** by refluxing the iron tricarbonyl complexes (−)-**1** and (−)-**7** (the latter synthesized in analogy to (−)-**1** from apopinene[10]) with an appropriate phosphine in cyclohexane (Scheme 1). In the case of (+)-**2**, the sluggish reaction called for a much longer reaction time. Thermal ligand exchange led in most cases to monophosphine complexes. The synthesis of a mixed diphosphine complex was attempted by photolyzing the triphenylphosphine complex (+)-**2** in the presence of trimethoxyphosphine. Surprisingly, a mixture of complexes (−)-**4** and (−)-**5** was obtained, containing, at the expense of triphenylphosphine, one and two trimethoxyphosphine ligands, respectively. Preliminary experiments showed that photolysis of complex (+)-**2** liberates triphenylphosphine even in the presence of CO, producing complex (−)-**1** in this case. The driving force for the substitution of a triphenylphosphine by a trimethoxyphosphine ligand lies in the smaller cone angle[11] of the latter. Using the even more slender phosphine ETPB (4-ethyl-2,6,7-trioxa-1-phosphabicyclo[2.2.2]octane), disubstitution partially occurred even under thermal conditions.

Structures. The structures of the complexes were determined by spectroscopic means and, in selected cases, by X-ray analysis (*cf.* Tables 2−5 and Figures 1−3). Although the hydrocarbon ligand of complex **3** seems to differ with respect to the other complexes discussed in this paper, it still belongs to exactly the same class with respect to its geometry, because the spatial arrangement around the iron center of all four coordinated (one σ- and three π-coordinated) carbon atoms in complex (+)-**2** is nearly identical with that in complex **3**: the best fit (using the program MacMoMo[12]) between these five-atom fragments leads to a largest deviation of only 0.07 Å. Variations of a similar order were noted between complexes (+)-**2** and (−)-**5**.

Table 1. Reductive Decomplexation of (+)-1, (+)-2, (−)-4, and (−)-5

starting material	L^1, L^2 (conditions)	ratio of products[a] 11	12	13	14	isolated yield, %
(+)-**1**	CO (*b*)	51	34	14	<1	93
(+)-**1**	CO (*c*)	20	25	55	<1	80
(+)-**1**	CO (*d*)	8	12	80	<1	61
(+)-**2**	CO, PPh_3 (*b*)	35	43	13	9	75
(−)-**4**	CO, $P(OMe)_3$ (*b*)	12	41	23	23	79
(−)-**5**	$P(OMe)_3$ (*b*)	*e*	*e*	22	78	85

[a] Determined by GC and/or NMR. [b] Conditions: room temperature, *hν*, neat HOAc. [c] Conditions: −40 °C, *hν*, 5% HOAc in diethyl ether. [d] Conditions: room temperature, *hν*, 2 equiv of HOAc in diethyl ether. [e] No traces detected.

Each of the two triphenylphosphine-substituted complexes (+)-**2** and **3** occurs as two independent molecules in the asymmetric unit, mostly differing in the orientation of the phenyl groups of the phosphine ligand.

Complexes (+)-**2**, (−)-**4**, and **6** show fluxional behavior in solution. The ^{1}H NMR spectrum of (+)-**2** remains broadened in most parts throughout the accessible temperature range of −50 to + 60 °C, due to at least two dynamic processes of different activation energy.

The high-temperature fluxionality might be due to interchange of CO and phosphine ligand positions (carbonyl rotation): even in complex (−)-**1** the three ^{13}C NMR signals for the different CO ligands appear as broadened lines (20 Hz at half-height at 126 MHz) at room temperature. In fact, careful inspection of the ^{1}H NMR spectrum of (+)-**2** reveals small additional peaks, first attributed to some impurity but later shown to be due to a slowly interchanging rotamer **C** of (+)-**2** (cf.

(10) Lightner, D. A.; Crist, B. V. *Tetrahedron* **1985**, *41*, 3021.
(11) Tolman, C. A. *Chem. Rev.* **1977**, *77*, 313.
(12) Dobler, M. Laboratorium für organische Chemie, ETH Zentrum, CH-8092 Zürich, Switzerland.

Table 2. Crystal Data and Structure Refinement Details for (+)-2, 3, and (−)-5

	(+)-**2**	**3**	(−)-**5**
empirical formula	$C_{30}H_{31}FeO_2P$	$C_{28}H_{27}FeO_2P$	$C_{17}H_{34}FeO_7P_2$
fw	510.37	482.35	468.25
temp (K)			193(2)
wavelength (Å)	0.71073	0.71073	0.71073
cryst size (mm)	0.75 × 0.38 × 0.15	0.47 × 0.42 × 0.17	0.57 × 0.57 × 0.53
cryst mounting		sealed glass cap	
cryst syst	triclinic	triclinic	orthorhombic
space group	*P*1	$P\bar{1}$	$P2_12_12_1$
unit cell dimens			
a (Å)	8.617(3)	10.485(2)	8.837(1)
b (Å)	9.591(3)	13.337(2)	14.415(1)
c (Å)	15.899(7)	16.743(3)	17.072(1)
α (deg)	84.36(5)	94.56(1)	0
β (deg)	86.95(3)	99.64(1)	90
γ (deg)	89.22(2)	91.48(1)	90
V (Å^3)	1305.7(8)	2299.1(7)	2174.7(3)
Z	2	4	4
calcd density (Mg m^{-3})	1.298	1.393	1.430
abs coeff (mm^{-1})	0.663	0.74	0.874
F(000)	560	1010	992
θ range for data collection (deg)	2.13−25.00		1.85−24.98
index ranges	$-10 \le h \le 10$	$-12 \le h \le 12$	$0 \le h \le 10$
	$-11 \le k \le 11$	$0 \le k \le 15$	$0 \le k \le 17$
	$0 \le l \le 18$	$-19 \le l \le 19$	$0 \le l \le 20$
no. of rflns collected	4583	8089	2195
no. of obsd rflns ($I > 2\sigma(I)$)	3944	6469	2091
no. of variables	619	577	245
R1[a]	0.049	0.043	0.032
wR2[b]	0.142	0.109	0.085
abs structure param	0.00(2)		0.03(2)
extinction coeff	0	0	0.0042(6)
goodness of fit on F^2	1.094	1.067	1.083
largest diff peak and hole (e Å^{-3})	0.803, −0.381	0.61, −0.50	0.73, −0.25

[a] $R1(\text{obsd data}) = \sum||F_o| - |F_c||/\sum|F_o|$. [b] $wR2(\text{all data}) = [\sum w(F_o^2 - F_c^2)^2/\sum wF_o^4]^{1/2}$.

Table 3. Selected Bond Lengths (Å) and Angles (deg) for (+)-2

	molecule A	molecule B		molecule A	molecule B
Fe(1)−P(1)	2.240(2)	2.243(2)	C(2)−C(7)	1.525 (11)	1.520(11)
Fe(1)−C(1)	2.103(8)	2.083(9)	C(3)−C(4)	1.513(12)	1.525(14)
Fe(1)−C(4)	2.236(7)	2.229(8)	C(4)−C(5)	1.388(11)	1.360(13)
Fe(1)−C(5)	2.135(7)	2.128(7)	C(5)−C(6)	1.380(11)	1.411(11)
Fe(1)−C(6)	2.151(7)	2.155(7)	C(5)−C(8)	1.514(12)	1.493(13)
Fe(1)−C(11)	1.740(8)	1.735(9)	C(6)−C(7)	1.525(11)	1.511(11)
Fe(1)−C(12)	1.768(9)	1.803(10)	O(1)−C(11)	1.154(11)	1.171(11)
C(1)−C(2)	1.521(11)	1.527(12)	O(2)−C(12)	1.164(11)	1.122(12)
C(2)−C(3)	1.515(13)	1.494(13)			
P(1)−Fe(1)−C(1)	89.1(2)	89.5(2)	C(5)−Fe(1)−C(12)	83.1(4)	83.1(4)
P(1)−Fe(1)−C(4)	97.0(2)	97.1(2)	C(6)−Fe(1)−C(11)	94.8(4)	94.2(4)
P(1)−Fe(1)−C(5)	128.6(2)	128.0(2)	C(6)−Fe(1)−C(12)	98.0(3)	98.3(4)
P(1)−Fe(1)−C(6)	161.2(2)	161.2(2)	C(11)−Fe(1)−C(12)	92.7(5)	92.6(5)
P(1)−Fe(1)−C(11)	101.3(3)	101.7(3)	Fe(1)−C(1)−C(2)	102.7(5)	103.1(6)
P(1)−Fe(1)−C(12)	90.9(3)	91.0(3)	C(1)−C(2)−C(3)	103.8(6)	103.9(7)
C(1)−Fe(1)−C(4)	80.4(3)	80.4(4)	C(1)−C(2)−C(7)	108.6(6)	108.7(7)
C(1)−Fe(1)−C(5)	99.4(3)	99.2(3)	C(3)−C(2)−C(7)	112.0(7)	112.8(8)
C(1)−Fe(1)−C(6)	82.9(3)	82.1(3)	C(2)−C(3)−C(4)	108.8(6)	108.2(6)
C(1)−Fe(1)−C(11)	84.2(4)	84.1(4)	C(3)−C(4)−C(5)	119.1(7)	119.8(7)
C(1)−Fe(1)−C(12)	176.8(4)	176.7(5)	C(4)−C(5)−C(6)	116.7(7)	116.4(7)
C(4)−Fe(1)−C(5)	36.9(3)	36.3(4)	C(4)−C(5)−C(8)	120.0(8)	120.0(9)
C(4)−Fe(1)−C(6)	64.9(3)	65.0(3)	C(6)−C(5)−C(8)	123.3(8)	123.6(9)
C(4)−Fe(1)−C(11)	155.8(4)	155.5(4)	C(5)−C(6)−C(7)	119.7(6)	119.0(7)
C(4)−Fe(1)−C(12)	102.8(4)	102.8(5)	C(2)−C(7)−C(6)	106.2(6)	105.6(6)
C(5)−Fe(1)−C(6)	37.6(3)	38.5(3)	Fe(1)−C(11)−O(1)	177.0(9)	176.7(10)
C(5)−Fe(1)−C(11)	129.8(4)	130.1(4)	Fe(1)−C(12)−O(2)	175.9(10)	174.4(12)

Scheme 2). Irradiating at either of the two additional peaks attributed to the proton atoms at the allylic moiety of rotamer **2C** leads to considerable saturation of the corresponding resonances of the prevailing rotamer **2A** (cf. Figure 4): i.e., irradiation at 4.16 ppm produces a saturation peak at 3.46 ppm (assigned to H−C(3′)) and saturating the line at 3.82 ppm affects the signal at 3.50 ppm (assigned to H−C(5′)). We therefore assign the small signals at 4.16 and 3.82 ppm to H−C(3′) and H−C(5′) in rotamer **2C**, respectively. No evidence for rotamer **2B** is found in the spectrum. Either of the two saturation experiments produces, in addition, smaller effects at the positions of the second allylic proton of both the prevailing and the irradiated minor isomer, however. This effect must be an artifact, since repeating the same experiment on complex **1** produces

Table 4. Selected Bond Lengths (Å) and Angles (deg) for 3

	molecule A	molecule B		molecule A	molecule B
Fe(1)−P(1)	2.2781(9)	2.2608(10)	C(2)−C(3)	1.529(5)	1.532(5)
Fe(1)−C(4)	2.122(3)	2.109(3)	C(3)−C(4)	1.519(5)	1.518(5)
Fe(1)−C(1)	2.154(3)	2.170(3)	C(4)−C(5)	1.525(5)	1.533(5)
Fe(1)−C(8)	2.056(3)	2.047(3)	C(5)−C(6)	1.513(5)	1.525(5)
Fe(1)−C(7)	2.176(3)	2.158(3)	C(6)−C(7)	1.521(5)	1.524(5)
Fe(1)−C(9)	1.763(3)	1.769(4)	C(7)−C(8)	1.406(5)	1.412(5)
Fe(1)−C(10)	1.757(3)	1.757(3)	O(9)−C(9)	1.154(4)	1.144(4)
C(1)−C(2)	1.526(5)	1.522(5)	O(10)−C(10)	1.151(4)	1.157(4)
C(1)−C(8)	1.404(5)	1.405(5)			
P(1)−Fe(1)−C(4)	172.8(1)	175.9(1)	C(8)−Fe(1)−C(10)	129.7(1)	128.9(1)
P(1)−Fe(1)−C(1)	97.4(1)	101.9(1)	C(7)−Fe(1)−C(9)	91.3(1)	91.6(1)
P(1)−Fe(1)−C(8)	86.7(1)	85.8(1)	C(7)−Fe(1)−C(10)	157.3(1)	158.8(1)
P(1)−Fe(1)−C(7)	106.1(1)	100.4(1)	C(9)−Fe(1)−C(10)	102.9(1)	102.8(1)
P(1)−Fe(1)−C(9)	96.9(1)	91.2(1)	C(2)−C(1)−C(8)	124.8(3)	125.8(3)
P(1)−Fe(1)−C(10)	89.9(1)	94.9(1)	C(1)−C(2)−C(3)	112.0(3)	111.6(3)
C(1)−Fe(1)−C(4)	82.5(1)	81.9(1)	C(2)−C(3)−C(4)	113.2(3)	112.3(3)
C(4)−Fe(1)−C(8)	97.6(1)	98.2(1)	Fe(1)−C(4)−C(3)	108.1(2)	108.8(2)
C(4)−Fe(1)−C(7)	80.8(1)	82.2(1)	Fe(1)−C(4)−C(5)	107.9(2)	107.3(2)
C(4)−Fe(1)−C(9)	85.1(1)	85.6(1)	C(3)−C(4)−C(5)	114.7(3)	114.3(3)
C(4)−Fe(1)−C(10)	82.8(1)	83.4(1)	C(4)−C(5)−C(6)	109.9(3)	110.7(3)
C(1)−Fe(1)−C(8)	38.9(1)	38.8(1)	C(5)−C(6)−C(7)	111.3(3)	111.1(3)
C(1)−Fe(1)−C(7)	70.1(1)	70.4(1)	C(6)−C(7)−C(8)	125.9(3)	124.0(3)
C(1)−Fe(1)−C(9)	159.0(1)	159.3(1)	C(1)−C(8)−C(7)	124.3(3)	124.8(3)
C(1)−Fe(1)−C(10)	92.4(1)	92.2(1)	Fe(1)−C(9)−O(9)	176.4(3)	177.7(3)
C(7)−Fe(1)−C(8)	38.7(1)	39.1(1)	Fe(1)−C(10)−O(10)	176.1(3)	176.9(3)
C(8)−Fe(1)−C(9)	127.3(1)	128.3(1)			

Table 5. Selected Bond Lengths (Å) and Angles (deg) for (−)-5

Fe(1)−C(7)	2.109(4)	C(1)−C(6)	1.514(6)
Fe(1)−C(3)	2.188(4)	C(2)−C(3)	1.413(6)
Fe(1)−C(2)	2.080(4)	C(2)−C(8)	1.506(6)
Fe(1)−C(1)	2.163(4)	C(3)−C(4)	1.496(6)
Fe(1)−C(17)	1.761(4)	C(4)−C(5)	1.519(6)
Fe(1)−P(1)	2.1476(12)	C(5)−C(6)	1.543(6)
Fe(1)−P(2)	2.1503(12)	C(5)−C(7)	1.525(6)
C(1)−C(2)	1.406(6)	O(7)−C(17)	1.152(5)
P(1)−Fe(1)−P(2)	109.06(5)	C(2)−Fe(1)−C(17)	86.7(2)
P(1)−Fe(1)−C(1)	154.58(12)	C(3)−Fe(1)−C(7)	81.1(2)
P(1)−Fe(1)−C(2)	124.02(13)	C(3)−Fe(1)−C(17)	104.7(2)
P(1)−Fe(1)−C(3)	89.70(11)	C(7)−Fe(1)−C(17)	173.0(2)
P(1)−Fe(1)−C(7)	86.11(12)	C(2)−C(1)−C(6)	119.1(4)
P(1)−Fe(1)−C(17)	89.92(14)	C(1)−C(2)−C(3)	115.8(4)
P(2)−Fe(1)−C(1)	93.05(12)	C(1)−C(2)−C(8)	123.3(4)
P(2)−Fe(1)−C(2)	126.33(13)	C(3)−C(2)−C(8)	120.8(5)
P(2)−Fe(1)−C(3)	158.64(12)	C(2)−C(3)−C(4)	120.0(4)
P(2)−Fe(1)−C(7)	89.85(12)	C(3)−C(4)−C(5)	108.9(3)
P(2)−Fe(1)−C(17)	85.98(14)	C(4)−C(5)−C(6)	111.2(4)
C(1)−Fe(1)−C(2)	38.6(2)	C(4)−C(5)−C(7)	104.4(4)
C(1)−Fe(1)−C(3)	66.6(2)	C(6)−C(5)−C(7)	108.0(3)
C(1)−Fe(1)−C(7)	81.4(2)	C(1)−C(6)−C(5)	106.1(3)
C(1)−Fe(1)−C(17)	104.4(2)	Fe(1)−C(7)−C(5)	102.8(3)
C(2)−Fe(1)−C(3)	38.6(2)	Fe(1)−C(17)−O(7)	176.1(4)
C(2)−Fe(1)−C(7)	100.3(2)		

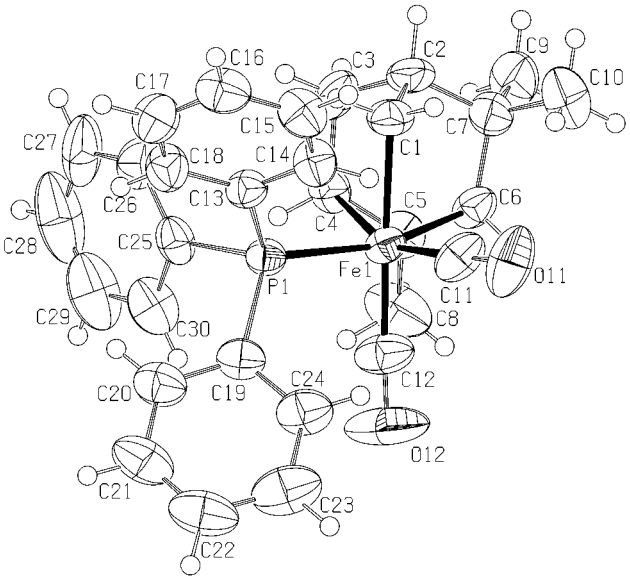

Figure 1. Perspective view of (+)-**2** (thermal ellipsoids at 50% probability level).

a similar saturation transfer between the allylic proton resonances only in the presence of paramagnetic impurities in the sample, but not in the case of well-resolved spectra.

The additional resonances attributed to rotamer **2C** "disappear" either on warming, by enhancing its exchange rate with the major rotamer and hence merging of the signals, or on cooling, by depletion due to the fairly large enthalpy difference between the rotamers ($\Delta G° \approx 6$ kJ/mol at room temperature).

The low-temperature fluxionality (or fluxionalities) of (+)-**2**, which includes excessive broadening and notable linear shifts of all ^{1}H NMR signals ($\Delta\delta$ ranging between +0.1 ppb/K (for H−C(3′)) and +3.7 ppb/K (for H−C(5′)); average for all signals +1.7 ppb/K), is more difficult to interpret (cf. Figure 5). The slow exchange limit of the process was not reached, due to rapidly decreasing solubility at temperatures below −50 °C thereby precluding further interpretations.

We conclude that an axial position for the phosphine ligand in σ-alkyl−π-allyl complexes of the type discussed in this paper is generally favored electronically (as shown by the structure of **3**) but to a great extent is disfavored by sterical hindrance from substituents, such as the methyl group at C(4) in the case of complex (+)-**2** at the central carbon atom of the π-allylic moiety. This conclusion is confirmed by the structure of the parent complex (−)-**8**, devoid of this methyl group. The apical position of the phosphine ligand in the latter compound was deduced among other arguments from the very similar chemical shifts and the identical J_{PC} splittings of the signals of the two remaining CO ligands.

All assigned resonances in the NMR spectra were attributed on the basis of completely analyzed ^{1}H and

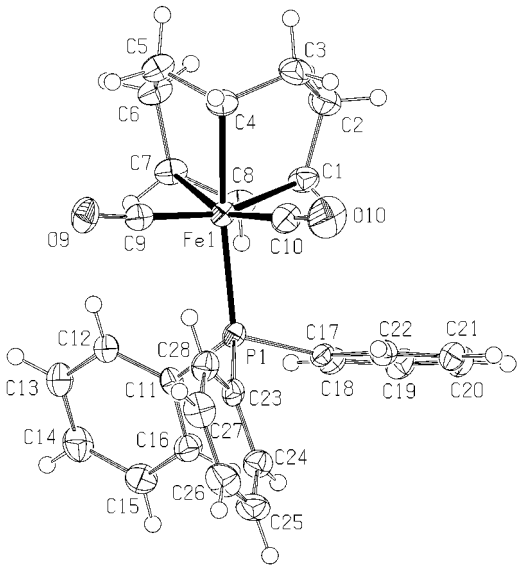

Figure 2. Perspective view of **3** (thermal ellipsoids at 50% probability level).

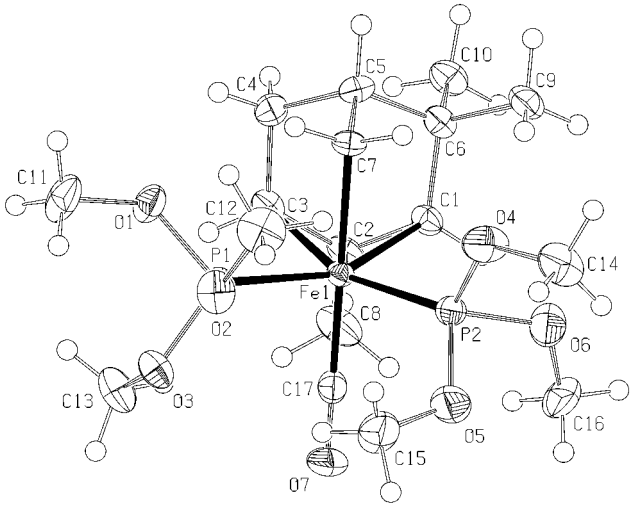

Figure 3. Perspective view of (−)-**5** (thermal ellipsoids at 50% probability level).

Scheme 2

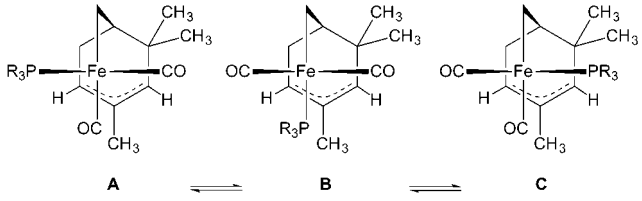

^{13}C NMR spectra, including homo- and heteronuclear shift correlation spectroscopy as well as selected NOE and homo- and heteronuclear decoupling experiments.

The different orientations of the phosphine ligands, i.e. axial or equatorial, translate also into very different scalar coupling constants between the ^{31}P nuclei of the phosphines and the ^{1}H and ^{13}C resonances of the hydrocarbon ligand. Comparison of the two structurally related complexes **3** and (−)-**8** reveal the capricious behavior of these coupling constants: in both compounds the σ-bonded carbon atoms couple (to a very different extent) to phosphorus, whereas the resonances of all direct substituents of these carbon atoms show

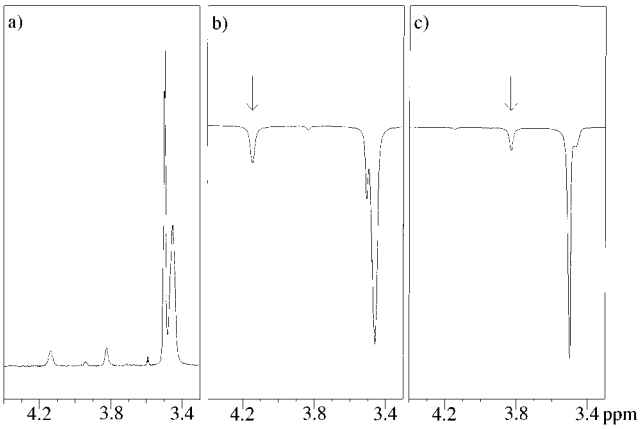

Figure 4. ^{1}H NMR spectrum (allylic proton region) of (a) (+)-**2** in $CDCl_3$ at room temperature and (b, c) saturation transfer difference spectra, irradiated at 4.16 and 3.82 ppm, respectively.

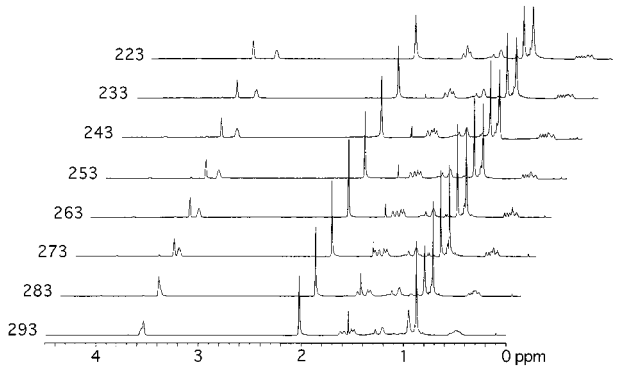

Figure 5. Variable-temperature ^{1}H NMR spectra of (+)-**2** in CD_2Cl_2.

no splitting. Coupling with phosphorus is observed, however, to some of the more remote nuclei. This behavior becomes only reasonable if one considers the more or less straight P−Fe−C three-center unit as one bond in the coupling path: the missing couplings would then correspond to nulled $^{2}J_{PX}$ interactions and the long-range splittings to dihedral angle sensitive $^{3}J_{PX}$ coupling constants.

A similar picture emerges for the allylic part of the ligands: small coupling constants (∼0 Hz (**3**) and 2.0 Hz (**7**)) between phosphorus and the central carbon and zero for the terminal ones but very large for the hydrogen substituent at the central carbon (19.6 Hz (**3**) and 16.5 Hz (**8**)). Small values are found for the hydrogen substituents at the terminal carbons (∼1.3 Hz (**3**) and ∼0 Hz (**8**)) despite favorable dihedral angles (∼30°) between the C−H and Fe−P bond vectors.

The J_{PC} coupling constants observed for the other four phosphine complexes ((+)-**2**, (−)-**4**, (−)-**5**, and **6**) as well as the resolved J_{PH} splittings in (−)-**5** and **6** nicely fit to the model: as the phosphine ligands occupy equatorial positions, C(1) is spaced from phosphorus by two orthogonal bonds this time, showing in all cases large coupling constants, whereas C(1′) and both hydrogen atoms at C(1) reside at a dihedral-angle-sensitive three-bond distance. Distinct differences were noted between the $^{n}J_{PX}$ coupling constants for triphenylphosphine and trimethyl phosphite or ETPB complexes, the latter being systematically larger, a fact which is generally ob-

served.[13] This observation is paralleled by the Fe−P bond distances, which are shortest in the case of the bis(trimethyl phosphite) complex (−)-**5**.

The ^{31}P-coupled ^{13}C NMR spectrum of (−)-**5** could be analyzed in a straightforward first-order manner, because the chemical shift difference ($\Delta\delta$ = 2.60 ppm) between the two phosphorus nuclei is much larger than their mutual coupling constant ($^2J_{PP}$ = 32.5 Hz) at the field strength of the spectrometers used. No attempt was made, however, to determine for each observed $^nJ_{PX}$ coupling constant which of the two phosphorus nuclei produces it, although in most cases assignments are suggested by simple comparison with the related monophosphine complex (−)-**4**.

Reactivity. As already mentioned in the discussion of the synthesis of the complexes, thermally and photochemically induced ligand exchange among the monodentate ligands is possible for all complexes without disturbing the σ-alkyl−π-allyl complexed ligand. As expected, the phosphine-substituted complexes are more readily oxidized than the parent complex (−)-**1** and hence less stable in air. The bicyclic ketones (−)-**9** and (+)-**10**[14] are isolated in a 1:1 mixture as the major

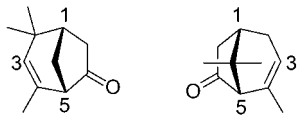

(-)-9 (+)-10

products from the oxidative degradation of (−)-**1** or any of its phosphie-substituted derivatives. These ketones are accompanied by small quantities of (−)-β-pinene. A mechanistic rationalization for this fact, which would also explain the complete absence of any (−)-α-pinene, cannot be given at the present time.

On treatment with $AlCl_3$ in the presence of CO, complex (−)-**1** yields a mixture of the same bicyclic ketones, but this time in a 94:6 regioselectivity in favor of (+)-**10**.[9] Use of the phosphine-substituted complex (+)-**2** in the same transformation leads to (+)-**10** exclusively. Subjecting the parent complex (−)-**8** to the same reaction conditions only led to complete destruction of the compound and not to the expected bicyclic ketones.

Photolysis of tricarbonyl iron complexes of dienes in neat acetic acid is known to lead to monoolefinic hydrocarbons or to aldehydes in the case of unconjugated ligands.[15] Surprisingly, complex (−)-**1** yields under these conditions a mixture of regioisomeric aldehydes **11** and **12**[9,16] and smaller amounts of the tetramethylcyclohexenes **13** and **14**[17] (cf. Table 1) accompanied by traces of the bicyclic ketones (−)-**9** and (+)-**10**. When the temperature of the reaction is lowered or the amount of added acetic acid is reduced, the cyclohexene **13** even becomes the major product. It is noteworthy that the observed ratio between the isomers **13** and **14** is in favor

Scheme 3. Mechanism of Reductive Photodecomplexation

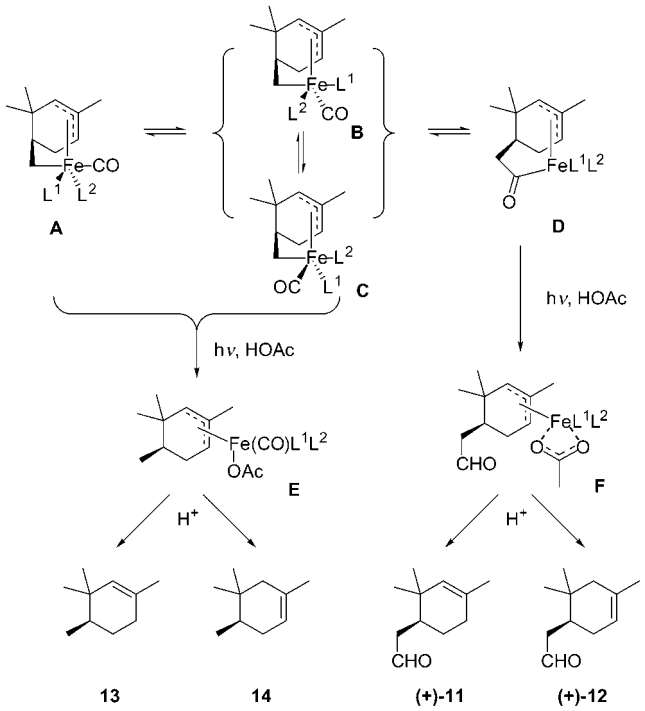

of the thermodynamically less stable one.[18] Applying the same treatment to the phosphine-substituted complexes (+)-**2** and (−)-**4** produces a similar result as in the case of (−)-**1**, except for selectivity changes within the pairs of isomers: the ratio between **11** and **12** switches from 60:40 to 45:55 and 23:77, respectively, whereas the selectivity for **13** drops from 14:1 to 1.5:1 and vanishes in the case of (−)-**4**. Reductive decomplexation of (−)-**5**, however, produces at the expense of the aldehydes only the cyclohexenes **13** and **14**, this time clearly in favor of the thermodynamically more stable **14**. As the aldehydes **11** and **12** are still present in the product mixture resulting from photolysis of (+)-**2** or (−)-**4**, but absent in the case of (−)-**5**, we conclude that their formation requires the presence of at least one equatorial CO ligand in the starting complex.

Mechanistically these selectivities could be explained as follows (cf. Scheme 3): any of the rotameric forms **A**, **B**, and **C** are protonated by acetic acid in the photoexcited state and subsequently yield intermediate **E**. This allylic complex is expected to be rapidly protolyzed to either **13** or **14**. In the case of carbonyl ligands this attack is directed predominantly to the less hindered C(5), whereas in the case of the electron-rich diphosphine complex **5** the attack predominantly occurs at the seemingly more hindered C(3) position, because steric repulsion between the geminal dimethyl group and the bulky iron moiety relocates the metal center more toward the less hindered C(5) end of the allylic system, shielding thereby C(5) and exposing C(3) to protonation by raising its electron density.

Formation of the aldehydes, however, requires the prior formation of the CO-inserted species **D**. Isomer **D** is not observed in the NMR spectra of any of the

(13) Sellin, M.; Luart, D.; Salaün, J.-Y.; Laurent, P.; des Abbayes, H. *J. Organomet. Chem.* **1998**, *562*, 183.
(14) Stockis, A.; Weissberger, E. *J. Am. Chem. Soc.* **1975**, *97*, 4288.
(15) Franck-Neumann, M.; Martina, D.; Brion, F. *Angew. Chem., Int. Ed. Engl.* **1978**, *17*, 690.
(16) An independent synthesis of *ent-**11*** has been reported: Wolleb, H.; Pfander, H. *Helv. Chim. Acta* **1986**, *69*, 646.
(17) An independent synthesis of *ent-**13*** and *ent-**14*** has been reported: Frater, G.; Helmlinger, D. *Helv. Chim. Acta* **1989**, *72*, 1515.
(18) Ab initio calculations (UHF/3-21G//UHF/3-21G and UHF/6-31G*//UHF/6-31G*) yield relative energy differences of 1.28 and 1.08 kJ/mol, respectively.

investigated complexes and is therefore assumed to be considerably higher in energy and hence only present in very small amounts in this solvent. The observed solvent effect for the aldehyde/olefin ratio (cf. Table 1) is explained by the lower stabilizing capacity of diethyl ether as compared to that of acetic acid, which reduces the formation of species **D** and hence the amount of aldehydes in the product mixture. In the case of diphosphine complex **5** its formation becomes unlikely for another reason: the required prior formation of either rotamer **B** or **C** is very unlikely to occur, due to steric repulsion between the C(4) methyl group and a bulky phosphine ligand in the apical position. The small amount of **D** present is presumably compensated by a faster reaction (higher quantum yield) and/or a better light absorption as compared to the parent complex. Not surprisingly, within a given set of ligands on iron the observed ratio of aldehydes always differs from the ratio between the olefins because of different ligand spheres of the intermediate species **E** and **F**.

Experimental Section

Reactions were performed under dry nitrogen or argon atmosphere, but the compounds were manipulated and handled in air. Solvents were nitrogen-saturated and dried. Reagents were used as obtained from commercial sources. Known procedures were applied for the carbonylation[9]/reductive decomplexation[15] reactions of (+)-**2**, (−)-**4**, (−)-**5**, and (−)-**8**. Photolyses were carried out using a high-pressure mercury light source (Philips HPK 125 W) through a Pyrex light filter. Melting points were determined by using a Kofler microapparatus (Reichert Thermovar) equipped with a digital thermometer. Optical rotations were measured with a Perkin-Elmer 241 MC polarimeter. Circular dichroism was measured on a Jobin Yvon Mark V dichrograph. Infrared spectra were measured on a Mattson 5010 FT-IR spectrometer. ^{1}H, ^{13}C, and ^{31}P NMR spectra were recorded on Bruker spectrometers (AM-360 or Avance DRX-500) at 360.13 or 500.13, 90.56 or 125.75, and 145.78 or 202.46 MHz, respectively. Chemical shifts (δ, ppm) were determined, if not stated otherwise, relative to internal TMS (^{1}H, ^{13}C), or external 85% H_3PO_4 (^{31}P). All signal assignments are based on NOE, COSY, and HETCOR experiments. The complex ^{1}H NMR spectrum of the mixture of **13** and **14** was analyzed using a *J*-resolved experiment.[19] Mass spectra were taken on a VG 70/70E instrument either with EI or CI (CH_4) ionization (70 eV) at a source temperature of 300 °C or with the FAB technique using an NBA matrix and a Xe gun.

(1′*R*)-Tricarbonyl[(3′-5′-η,1-σ)-methylene(2,2,4-trimethyl-4-cyclohexene-1,3-diyl)]iron ((−)-1).[9] A mixture of (−)-β-pinene (95.1% ee by chiral capillary GC (Supelco β-dex 110); 36.0 g, 0.264 mol) and iron pentacarbonyl (54 mL, 0.4 mol) in dioxane (100 mL) and heptane (20 mL) was heated to reflux for 3 days using a Dean−Stark trap filled with molecular sieves (3 Å). The reaction mixture was filtered through a plug of alumina, the solvents, unreacted β-pinene, and small amounts of (−)-**9** and (+)-**10** (∼2% each) were removed in vacuo, and the remaining oil was purified by distillation (76 °C, 0.2 mbar) yielding 45.9 g of (−)-**1** (63%).

Yellow oil. $[\alpha]^{20}_D = -68.8°$ (c = 1.002, *n*-pentane). CD (6×10^{-2} M, *n*-pentane; $\Delta\epsilon$ (λ, nm)): −1.0 (320). FT-IR (film, cm^{-1}): ν(C≡O) 2042 (vs), 1970 (vs). ^{1}H NMR (500 MHz, $CDCl_3$): δ 4.10 (dddd, J = 4.3, 2.1, 1.8, 1.2, H−C(5′)), 4.04 (dd, J = 2.1, 1.8 Hz, H−C(3′)), 2.05 (ddt, J = 14.3, 2.9, 1.8 Hz, H_{exo}−C(6′)), 1.89 (br s, H_3C−C(4′)), 1.59 (dt, J = 9.7, 2.9 Hz, H_{pro-S}−C(1)), 1.52 (dddt, J = 3.6, 2.9, 2.4, 1.8 Hz, H−C(1′)), 1.28 (ddd, J = 14.3, 4.3, 3.6 Hz, H_{endo}−C(6′)), 1.09 (dd, J = 9.7, 2.4 Hz, H_{pro-R}−C(1)), 0.94 (s, 6 H, $(H_3C)_2$−C(2′)). ^{13}C NMR (126 MHz, $CDCl_3$): δ 216.9, 215.5, and 207.2 (3s, C≡O), 103.4 (s, C(4′)), 87.2 (d, C(3′)), 76.8 (d, C(5′)), 49.1 (d, C(1′)), 40.3 (s, C(2′)), 33.8 (t, C(1)), 33.7 (t, C(6′)), 28.1, 0 (q, $C_{exo}(2'^1)$), 27.2 (q, C(4′^{1})), 27.0 (q, $C_{endo}(2'^1)$).

(1′*R*)-Dicarbonyl[(3′-5′-η,1-σ)-methylene(2,2,4-trimethyl-4-cyclohexene-1,3-diyl)](triphenylphosphine)iron ((+)-2). A mixture of (−)-**1** (1.0 g, 3.6 mmol) and triphenylphosphine (0.95 g, 3.6 mmol) in cyclohexane (10 mL) was heated to reflux for 4 h. The solvent was removed in vacuo, and the remaining oil was purified by column chromatography using *n*-pentane/dichloromethane (1:1) as the eluant. The yellow band was collected, yielding 1.48 g of (+)-**2** (80%). Further purification was achieved by recrystallization from dry methanol, free of acetone, until a constant rotation was obtained.

Yellow crystals. Mp: 101−104 °C. Anal. Calcd for $C_{30}H_{31}FeO_2P$: C, 70.60; H, 6.12. Found: C, 71.17; H, 6.20. $[\alpha]^{20}_D$ = +114° (c = 0.85, *n*-hexane);. CD (3.05×10^{-4} M, *n*-hexane; $\Delta\epsilon$ (λ, nm)): +3.5 (359), +1.5 (325, shoulder), −2.7 (291). FT-IR (*n*-pentane, cm^{-1}): ν(C≡O) 1981.0 (vs), 1928.5 (vs). ^{1}H NMR (360 MHz, C_6D_6): δ 7.66 and 7.00 (2m, 6 and 9 H, respectively, phenyl), 3.50 (br, H−C(3′)), 3.48 (br, H−C(5′)), 1.97 (s, H_3C−C(4′)), 1.93 (br d, J = 9.7 Hz, H_a−C(1)), 1.67 (br d, J = 13.8 Hz, H_a−C(6′)), 1.45 (br, H−C(1′)), 1.16 (s, H_3C_{endo}−C(2′)), 0.89 (s, H_3C_{exo}−C(2′)), 0.84 (br dd, J_{PH} = 17.7 Hz, J = 9.7 Hz, H_b−C(1)), 0.66 (br d, J = 13.8 Hz, H_b−C(6′)). ^{13}C NMR (91 MHz, 273 K, CD_2Cl_2): δ 224.0 and 212.8 (2d, J_{PC} = 5.7 and 20.6 Hz, respectively, C≡O), 136.9 (d, J_{PC} = 37.9 Hz, C(1″)), 133.3 (dd, J_{PC} = 9.9 Hz, C(2″,6″)), 129.5 (d, C(4″)), 128.2 (dd, J_{PC} = 8.9 Hz, C(3″,5″)), 101.7 (s, C(4′)), 80.0 (dd, J_{PC} = 5.6 Hz, C(3′)), 79.1 (dd, J_{PC} = 9.7 Hz, C(5′)), 49.1 (d, C(1′)), 41.3 (s, C(2′)), 37.1 (*t*d, J_{PC} = 17.8 Hz, C(1)), 31.6 (t, C(6′)), 27.9, 27.3 and 27.0 (3q, C(2′^{1}, 4′^{1})). ^{31}P NMR (146 MHz, C_6D_6): δ 83.0. CI-MS (*m*/*z* (rel intensity)): 511 (8, MH^+), 510 (8, M^+), 483 (25, $MH^+ - CO$), 482 (54, $M^+ - CO$), 455 (35, $MH^+ - 2\,CO$), 454 (49, $M^+ - 2\,CO$), 263 (100, $HPPh_3^+$).

Dicarbonyl((4−6-η,1-σ)-cyclooctenediyl)(triphenylphosphine)iron (3). Complex **3** was synthesized by following a literature procedure.[2b] Suitable crystals were grown from *n*-pentane/diethyl ether (9:1).

^{1}H NMR (500 MHz, $CDCl_3$): δ 7.41 and 7.37 (2m, 15 H, phenyl), 4.37 (tdd, J = 8.0, 4.6 Hz, J_{PH} = 1.3 Hz, H−C(4,6)), 3.78 (dt, J_{PH} = 19.6 Hz, J = 8.0 Hz, H−C(5)), 2.61 (m, H_{endo}−C(2,8)), 2.60 (m, H−C(1)), 2.01 (m, H_{endo}−C(3,7)), 1.64 (m, H_{exo}−C(3,7)), 1.55 (m, J_{PC} = 8.4 Hz, H_{exo}−C(2,8)). ^{13}C NMR (126 MHz, $CDCl_3$): δ 222.9 (d, J_{PC} = 15.0 Hz, C≡O), 134.4 (d, J_{PC} = 32.9 Hz, C(1′)), 132.8 (dd, J_{PC} = 10.3 Hz, C(2′,6′)), 129.7 (d, C(4′)), 128.3 (dd, J_{PC} = 8.8 Hz, C(3′,5′)), 93.1 (d, C(5)), 86.4 (d, C(4,6)), 50.3 (t, C(2,8)), 49.8 (dd, J_{PC} = 22.6 Hz, C(1)), 27.6 (td, J_{PC} = 5.4 Hz, C(3,7)). ^{31}P NMR (202 MHz, $CDCl_3$): δ 56.1.

(1′*R*)-Dicarbonyl[(3′-5′-η,1-σ)-methylene(2,2,4-trimethyl-4-cyclohexene-1,3-diyl)](trimethoxyphosphine)iron ((−)-4). A. A mixture of (−)-**1** (312 mg, 1.13 mmol) and trimethoxyphosphine (0.28 mL, 2.26 mmol) in cyclohexane (10 mL) was heated to reflux for 4 h. After removal of the solvent and excess phosphine under reduced pressure, the product mixture was eluted on silica gel with *n*-pentane to remove unreacted (−)-**1**. Further elution with *n*-pentane/dichloromethane (1:1) yielded 210 mg of (−)-**4** (50%) as a yellow oil.

B. A mixture of (−)-**1** (500 mg, 1.8 mmol) and trimethoxyphosphine (250 mg, 2 mmol) in *n*-pentane (50 mL) were photolyzed with a high-pressure mercury lamp (Pyrex filter) for 2 h. After removal of the solvent and excess phosphine under reduced pressure, the product mixture was eluted on silica gel with *n*-pentane to remove unreacted (−)-**1** (72 mg, 0.26 mmol) and phosphine. On further elution with *n*-pentane/dichloromethane (1:1) two yellow bands are separated. The first one yields 366 mg of (−)-**4** (54%) and the second one 50

(19) Aue, W. P.; Karhan, J.; Ernst, R. R. *J. Chem. Phys.* **1976**, *64*, 4226.
(20) Sheldrick, G. M. SHELXS-86. *Acta Crystallogr.* **1990**, *A46*, 467.

mg of (−)-**5** (11%). Recrystallization from dry methanol (until constant rotation) yielded an analytically pure sample.

Anal. Calcd for $C_{15}H_{25}FeO_5P$: C, 48.41; H, 6.77. Found: C, 48.92; H, 6.84. $[\alpha]^{20}_D = -168°$ (c = 1.05, n-pentane). CD (4.78 × 10^{-4} M, n-hexane; $\Delta\epsilon$ (λ, nm)): +1.1 (333), −0.8 (302). FT-IR (n-pentane, cm^{-1}): ν(C≡O) 1984.3 (vs), 1926.3 (vs). ^{1}H NMR (500 MHz, C_6D_6): δ 4.10 (br m, H−C(5′)), 3.72 (br, H−C(3′)), 3.29 (d, J_{PH} = 11.1 Hz, OCH_3), 1.98 (br d, J = 13.1 Hz, H_a−C(6′)), 1.81 (s, H_3C−C(4′)), 1.60 (br, H_a−C(1)), 1.59 (br m, H−C(1′)), 1.40 (br d, J = 13.1 Hz, H_b−C(6′)), 1.29 (br dd, J = 13.6, 8.9 Hz, H_b−C(1)), 1.11 and 0.95 (2s, H_3C−C(2′)). ^{13}C NMR (126 MHz, 233 K, $CDCl_3$): δ 222.3 and 210.5 (2d, J_{PC} = 8.5 and 27.9 Hz, respectively, C≡O), 100.4 (s, C(4′)), 83.3 (dd, J_{PC} = 15.5 Hz, C(3′)), 72.1 (dd, J_{PC} = 8.5 Hz, C(5′)), 51.4 (qd, J_{PC} = 3.0 Hz, OCH_3), 48.0 (d, C(1′)), 39.9 (d, J_{PC} = 2.0 Hz, C(2′)), 32.0 (t, C(6′)), 29.9 (*t*d, J_{PC} = 29.9 Hz, C(1)), 28.2 (q, $C_a(2'^1)$), 27.4 (q, C(4′^{1})), 26.8 (q, $C_b(2'^1)$). ^{31}P NMR (146 MHz, $CDCl_3$): δ 184.4; EI-MS (m/z (rel intensity)): 372 (0.4, M^+), 344 (4, M^+ − CO), 316 (13, M^+ − 2 CO), 192 (30, M^+ − 2 CO − $P(OMe)_3$), 93 (100, $P(OMe)_2^+$).

(1′*R*)-Carbonyl[(3′−5′-*η*,1-*σ*)-methylene(2,2,4-trimethyl-4-cyclohexene-1,3-diyl)]bis(trimethoxyphosphine)iron ((−)-5). A mixture of (−)-**1** (500 mg, 1.8 mmol) and trimethoxyphosphine (470 mg, 3.8 mmol) in n-pentane (50 mL) was photolyzed for 10 h. After removal of the solvent and excess phosphine under reduced pressure, the product mixture was eluted on silica gel with n-pentane/dichloromethane (1:1) to remove small amounts of unreacted (−)-**1**, (−)-**4**, and phosphine. Elution of the yellow band yielded 636 mg (−)-**5** (75%) as a yellow powder. Recrystallization from dry methanol gave 483 mg (57%) of analytically pure compound.

Yellow crystals. Mp: 108.5−111.0 °C. Anal. Calcd for $C_{17}H_{34}FeO_7P_2$: C, 43.61; H, 7.32. Found: C, 43.77; H, 7.46. $[\alpha]^{20}_D$ = −378° (c = 0.9, n-hexane). CD (3.59 × 10^{-4} M, n-hexane; $\Delta\epsilon$ (λ, nm)): −0.96 (323), +0.01 (292), −0.46 (278). FT-IR (n-pentane, cm^{-1}): ν(C≡O) 1903.1 (vs). ^{1}H NMR (500 MHz, CD_2Cl_2, 293 K): δ 3.63 (br m, H−C(5′)), 3.62 and 3.59 (2d, J_{PH} = 10.4 and 10.6 Hz, respectively, OCH_3), 3.32 (dq, J = 4.3, 2.0 Hz, H−C(3′)), 1.92 (s, H_3C−C(4′)), 1.75 (br dd, J = 12.7, 5.4 Hz, H_a−C(6′)), 1.23 (ddq, J = 18.0, 9.5, 2.0 Hz, H_S−C(1)), 1.19 (m, H−C(1′)), 1.15 (dm, J = 12.7 Hz, H_b−C(6′)), 0.87 (s, H_3C_{exo}−C(2′)), 0.82 (s, H_3C_{endo}−C(2′)), 0.73 (ddm, J = 18.5, 9.5 Hz, H_R−C(1)). ^{13}C NMR (126 MHz, CD_2Cl_2): δ 214.2 (dd, J_{PC} = 35.4, 31.1 Hz, C≡O), 97.3 (s, C(4′)), 81.0 (dd, J_{PC} = 18.4, 9.8 Hz, C(3′)), 66.9 (dd, J_{PC} = 16.5, 9.4 Hz, C(5′)), 51.9 and 51.7 (2d, J_{PC} = 6.5 and 5.8 Hz, respectively, OCH_3), 49.2 (dd, J_{PC} = 1.7, 1.3 Hz, C(1′)), 40.2 (dd, J_{PC} = 2.6, 0.5 Hz, C(2′)), 33.1 (dd, J_{PC} = 3.0, 0.7 Hz, C(6′)), 28.7 (dd, J_{PC} = 4.1, 1.2 Hz, $C_{exo}(2'^1)$), 28.3 (dd, J_{PC} = 35.3, 28.3 Hz, C(1)), 27.6 (t, J_{PC} = 1.1 Hz, C(4′^{1})), 27.4 (s, $C_{endo}(2'^1)$). ^{31}P NMR (202 MHz, CD_2Cl_2): δ 186.5 and 183.9 (2d, J = 32.5 Hz). CI-MS (m/z (rel intensity)): 468 (23, M^+), 440 (21, M^+ − CO), 437 (35, M^+ − OCH_3), 344 (16, M^+ − $P(OMe)_3$), 316 (23, M^+ − CO − $P(OMe)_3$), 217 (65), 125 (100, $HP(OMe)_3^+$).

(1′*R*)-Dicarbonyl[(3′-5′-*η*,1-*σ*)-methylene(2,2,4-trimethyl-4-cyclohexene-1,3-diyl)](4-ethyl-2,6,7-trioxa-1-phosphabicyclo[2.2.2]octane)iron ((−)-6). A mixture of (−)-**1** (5.5 g, 20 mmol) and 4-ethyl-2,6,7-trioxa-1-phosphabicyclo[2.2.2]-octane (ETPB, 1.75 g, 11 mmol) in cyclohexane (100 mL) was heated to reflux for 6 h. After removal of a solid by filtration (500 mg, tentatively attributed to the corresponding bis-ETPB complex), the solvent and excess phosphine were evaporated under reduced pressure. The residual mixture was eluted on silica gel with n-pentane to remove unreacted (−)-**1** (3.92 g, 71%). Further elution with n-pentane/diethyl ether (8:2) yielded 550 mg of (−)-**6** (12%) as a pale yellow solid.

Anal. Calcd for $C_{18}H_{28}FeO_5P$: C, 52.57; H, 6.86. Found: C, 52.57; H, 6.70. ^{1}H NMR (500 MHz, CD_2Cl_2, 283 K): δ 4.22 (d, J = 4.7 Hz, OCH_2), 4.02 (br m, H−C(5′)), 3.81 (br, H−C(3′)), 1.87 (br d, J = 13.4 Hz, H_a−C(6′)), 1.81 (s, H_3C−C(4′)), 1.36 (br m, H−C(1′)), 1.22 (m, H_b−C(6′)), 1.21 (q, J = 7.7 Hz, CH_2-CH_3), 1.09 (br d, J = 9.8 Hz, H_a−C(1)), 1.04 (ddd, J = 16.7, 9.8, 2.0 Hz, H_b−C(1)), 0.90 (s, H_3C_a−C(2′)), 0.88 (s, H_3C_b−C(2′)), 0.81 (t, J = 7.7 Hz, CH_2CH_3). ^{13}C NMR (126 MHz, $CDCl_3$, 300 K): δ 220.0 and 210.0 (2d, J_{PC} = 9.7 and 28.7 Hz, respectively, C≡O), 101.4 (s, C(4′)), 83.7 (dd, J_{PC} = 17.0 Hz, C(3′)), 74.2 (td, J_{PC} = 6.9 Hz, OCH_2), 73.4 (dd, J_{PC} = 7.9 Hz, C(5′)), 48.9 (d, C(1′)), 40.1 (s, C(2′)), 34.9 (d, J_{PC} = 31.2 Hz, CEt), 32.5 (t, C(6′)), 30.1 (td, J_{PC} = 31.4 Hz, C(1)), 28.1 (q, $C_a(2'^1)$), 27.3 (q, C(4′^{1})), 27.1 (q, $C_b(2'^1)$), 23.5 (t, CH_2CH_3), 7.1 (q, CH_2CH_3).

(1′*R*)-Tricarbonyl[(3′-5′-*η*,1-*σ*)-methylene(2,2-dimethyl-4-cyclohexene-1,3-diyl)]iron ((−)-7). A mixture of (−)-apopinene[10] (1.22 g, 10 mmol) and $Fe(CO)_5$ (3.14 g, 16 mmol) in anhydrous dioxane (12 mL) containing n-heptane (6 mL) in a light-protected flask (lined with the iron deposit from a previous reaction of the same type) equipped with a Dean−Stark trap (filled with molecular sieves) topped by a reflux condenser was heated to reflux under N_2 (bath temperature 130 °C) for 24 h. After filtration through aluminoxane and removal of the solvents, unreacted starting materials, and some volatile byproducts by evaporation in vacuo (room temperature, 1 mbar), the product was purified by column chromatography (silica gel, n-pentane) to give 1.21 g (46%) of pure (−)-**7** as a pale yellow liquid.

Anal. Calcd for $C_{12}H_{14}FeO_3$: C, 54.99; H, 5.38. Found: C, 55.43; H, 5.59. $[\alpha]^{20}_D$ = −24.1° (c = 0.4, pentane). CD (5.55 × 10^{-4} M, n-pentane; $\Delta\epsilon$ (λ, nm)): −0.33 (319), +0.17 (280). FT-IR (film, cm^{-1}): ν(C≡O) 2051.2 (vs), 1987.5 (vs), 1983.0 (vs). ^{1}H NMR (500 MHz, $CDCl_3$): δ 4.74 (tm, J = 6.9 Hz, H−C(4′)), 4.58 (ddtd, J = 6.9, 4.5, 1.7, 1.3 Hz, H−C(5′)), 4.20 (dt, J = 7.0, 1.8 Hz, H−C(3′)), 2.07 (ddq, J = 14.6, 3.0 Hz, 1.6 Hz, H_{exo}−C(6′)), 1.53−1.63 (m, 2 H, H−C(1′), H_{pro-S}−C(1)), 1.24 (dt, J = 14.6 Hz, 3.9 Hz, H_{endo}−C(6′)), 1.09 (m, H_{pro-R}−C(1)), 1.00 (s, H_3C_{exo}−C(2′)), 0.93 (s, H_3C_{endo}−C(2′)). ^{13}C NMR (126 MHz, $CDCl_3$): δ 217.0, 215.5, and 207.3 (3s, C≡O), 86.7 (d, C(4′)), 85.9 (d, C(3′)), 76.3 (d, C(5′)), 50.2 (d, C(1′)), 38.7 (s, C(2′)), 32.5 (t, C(1)), 32.4 (t, C(6′)), 28.5 (q, $C_{exo}(2'^1)$), 27.0 (q, $C_{endo}(2'^1)$);. EI-MS (m/z (rel intensity)): 262 (7, M^+), 234 (34, M^+ − CO), 206 (29, M^+ − 2 CO), 178 (100, M^+ − 3 CO).

(1′*R*)-Dicarbonyl[(3′-5′-*η*,1-*σ*)-methylene(2,2-dimethyl-4-cyclohexene-1,3-diyl)](triphenylphosphine)iron ((−)-8). A mixture of (−)-**7** (0.53 g, 2.0 mmol) and triphenylphosphine (0.54 g, 2.0 mmol) in cyclohexane (15 mL) was heated to reflux for 6 h. The solvent was removed in vacuo, and the remaining oil was purified by column chromatography using n-pentane/dichloromethane (10:1) as the eluant. The yellow band following some unreacted starting material (0.12 g, 22%) was collected, yielding 0.42 g of (−)-**8** (42%) as yellow crystals. Further purification was achieved by recrystallization from ethanol.

Yellow crystals. Mp: 172 °C. Anal. Calcd for $C_{29}H_{29}FeO_2P$: C, 70.17; H, 5.89. Found: C, 69.71; H, 5.86. $[\alpha]^{20}_D$ = −15.1° (c = 0.4, $CHCl_3$). CD (3.11 × 10^{-4} M, $CHCl_3$; $\Delta\epsilon$ (λ, nm)): −0.24 (375). FT-IR (KBr, cm^{-1}): ν(C≡O) 1984.6 (vs), 1931.6 (vs). ^{1}H NMR (500 MHz, $CDCl_3$): δ 7.37 (m, 15 H, phenyl), 4.08 (dt, J_{PH} = 16.5 Hz, J = 6.8 Hz, H−C(4′)), 3.77 (ddq, J = 6.7, 4.3 Hz, 1.6 Hz, H−C(5′)), 3.53 (dt, J = 6.8, 1.9 Hz, H−C(3′)), 1.87 (dm, J = 14.0 Hz, H_{exo}−C(6′)), 1.73 (dt, J = 9.4, 2.8 Hz, H_{pro-S}−C(1)), 1.57 (m, J_{PH} = 2.2 Hz, H−C(1′)), 1.174 (dm, J = 9.4 Hz, H_{pro-R}−C(1)), 1.169 (*dt*, J = 14.0, 3.8 Hz, H_{endo}−C(6′)), 0.92 (s, H_3C_{endo}−C(2′)), 0.85 (s, H_3C_{exo}−C(2′)). ^{13}C NMR (126 MHz, $CDCl_3$): δ 223.5 and 222.3 (2d, J_{PC} = 18.1 Hz, each, C≡O), 135.1 (d, J_{PC} = 35.4 Hz, C(1″)), 132.7 (dd, J_{PC} = 10.4 Hz, C(2″,6″)), 129.7 (dd, J_{PC} = 2.0 Hz, C(4")), 128.3 (dd, J_{PC} = 9.0 Hz, C(3″,5″)), 86.1 (dd, J_{PC} = 2.0 Hz, C(4′)), 84.5 (d, C(3′)), 73.0 (d, C(5′)), 51.2 (d, C(1′)), 38.8 (d, J_{PC} = 2.9 Hz, C(2′)), 32.7 (td, J_{PC} = 2.4 Hz, C(6′)), 32.1 (td, J_{PC} = 16.8 Hz, C(1)), 28.7 (q, $C_{exo}(2'^1)$), 27.3 (q, $C_{endo}(2'^1)$). ^{31}P NMR (202 MHz, $CDCl_3$): δ 64.4. EI-MS (m/z (rel intensity)): 468 (0.5, M^+ − CO), 440 (3.3, M^+ − 2 CO), 318 (15, PPh_3Fe^+), 262 (61, PPh_3^+), 183 (100, $C_{12}H_8P^+$), 108 (63, PPh^+). FAB-MS (m/z (rel intensity)): 497

(4, MH^+), 496 (9, M^+), 495 (10, $(M - H)^+$), 468 (33, $M^+ - CO$), 440 (100, $M^+ - 2\ CO$), 318 (98, PPh_3Fe^+).

Carbonylation/Decomplexation of (+)-2. A solution of (+)-**2** (840 mg, 1.65 mmol) and Cu_2Cl_2 (160 mg, 1.62 mmol) in dichloromethane (20 mL) was purged for 1 min with CO at 0 °C. After addition of a solution of $AlCl_3$ (360 mg, 2.7 mmol) in dichloromethane (10 mL), the mixture was stirred at 0 °C for 24 h. Throughout the reaction the CO pressure was kept above 0.8 bar. Hydrolysis with ice−water followed by separation of the organic layer, drying with Na_2SO_4, removal of the solvent, and purification of the residue by column chromatography on silica gel (*n*-pentane/diethyl ether, 8:2) yields pure (+)-**10** (R_f 0.49, 70 mg, 26%). No trace of the isomeric ketone (−)-**9** (R_f 0.38) was found under these conditions.

(−)-(1′*S*)-2,4,4-Trimethylbicyclo[3.2.1]oct-3-en-6-one ((−)-9). Bp: 67−70 °C (1 mbar). $[\alpha]^{20}_D = -498.1°$ ($c = 0.37$, *n*-pentane; 96.8% ee by chiral capillary GC (Supelco β-dex 110)). CD (0.5 mM, diethyl ether; $\Delta\epsilon$ (λ, nm)): −10.5 (290), −11.5 (302), −7.0 (315). FT-IR (film, cm^{-1}) 2972 (s), 2879 (m), 1754 (vs), 1444 (w), 1172 (m). ^1H NMR (500 MHz, $CDCl_3$): δ 5.12 (quint, $J = 1.4$ Hz, H−C(3)), 2.44−2.48 (m, H_{endo}−C(7), H−C(5)), 2.13−2.00 (m, H_{exo}−C(7), H−C(1)), 2.08 (dd, $J = 11.6$ Hz, 3.7 Hz, H_{pro-R}−C(8)), 1.86 (dt, $J = 11.6$ Hz, 4.5 Hz, H_{pro-S}−C(8)), 1.68 (d, $J = 1.4$ Hz, H_3C−C(4)), 1.12 (s, H_3C_{exo}−C(2)), 0.98 (s, H_3C_{endo}−C(2)). ^{13}C NMR (126 MHz, $CDCl_3$): δ 211.7 (s, C(6)), 133.1 (d, C(3)), 130.4 (s, C(4)), 52.1 (d, C(5)), 42.1 (d, C(1)), 40.0 (t, C(7)), 36.4 (s, C(2)), 31.6 (t, C(8)), 30.3 (q, $C_{exo}(2^1)$), 25.7 (q, $C_{endo}(2^1)$), 22.5 (q, $C(4^1)$). EI-MS (*m*/*z* (rel intensity)): 164 (32, M^+), 149 (16), 131 (5), 122 (24), 121 (32), 120 (19), 107 (100), 105 (36), 95 (7), 93 (38), 91 (85), 79 (46), 77 (42), 67 (13), 65 (22), 53 (23), 51 (13), 42 (24), 41 (37), 39 (42).

(+)−(1′*S*)-4,8,8-Trimethylbicyclo[3.2.1]oct-3-en-6-one ((+)-10). Bp: 67−70 °C (1 mbar). $[\alpha]^{20}_D = +526.7°$ ($c = 0.37$, *n*-pentane; 96.6% ee by chiral capillary GC (Supelco β-dex 110)). CD (0.9 mM, diethyl ether; $\Delta\epsilon$ (λ, nm)): +10.5 (290), +11.5 (302), +7.0 (315). FT-IR (film, cm^{-1}): 2959 (*m*), 1744 (vs), 1443 (w), 1126 (w). ^1H NMR (500 MHz, $CDCl_3$): δ 5.42 (m, H−C(3)), 2.56 (ddd, $J = 18.6$, 7.1, 1.0 Hz, H_{exo}−C(7)), 2.46 (dm, $J = 19$ Hz, H_{exo}−C(2)), 2.25 (s, H−C(5)), 2.03 (d, $J = 18.6$ Hz, H_{endo}−C(7)), 1.88−1.95 (m, H_{endo}−C(2), H−C(1)), 1.70 (*d*t, $J = 2.4$, 1.6 Hz, H_3C−C(4)), 1.00 (s, H_3C_{pro-S}−C(8)), 0.97 (s, H_3C_{pro-R}−C(8)). ^{13}C NMR (126 MHz, $CDCl_3$): δ 211.3 (s, C(6)), 132.0 (s, C(4)), 121.5 (d, C(3)), 63.9 (d, C(5)), 43.3 (t, C(7)), 39.1 (d, C(1)), 37.7 (s, C(2)), 32.9 (t, C(2)), 27.0 (q, $C_{pro-R}(8^1)$), 22.9 (q, $C(4^1)$), 20.2 (q, $C_{pro-S}(8^1)$). EI-MS (*m*/*z* (rel intensity)): 164 (24, M^+), 149 (20), 131 (4), 122 (28), 121 (17), 120 (19), 107 (100), 105 (31), 95 (16), 93 (45), 91 (49), 79 (31), 77 (28), 67 (19), 65 (13), 53 (10), 51 (12), 42 (12), 41 (25), 39 (36).

Reductive Decomplexation of (+)-1. A solution of (+)-**1** (500 mg, 1.81 mmol) in degassed glacial acetic acid (50 mL) was irradiated at room temperature with a high-pressure mercury lamp (Pyrex filter) for 4 h. The resulting orange solution was extracted with pentane (3 × 20 mL), and the combined extracts were washed with water, dried over $MgSO_4$, and concentrated by distillation at atmospheric pressure. GC/MS of the crude product reveals the presence of three products (retention time (min)/mass (*m*/*z*)/intensity (%): 2.51/138/15, 6.88/166/51, 6.94/166/34). The first product was identified as **13** (see below) by its retention time and fragmentation pattern. Chromatography on silica gel (*n*-pentane/diethyl ether (8:2), $R_f = 0.46$) leads to an inseparable mixture of two aldehydes (235 mg, 78% yield) in a 55:45 ratio according to capillary GC and ^1H NMR, identified by NMR as (1′*S*)-2-(2,2,4-trimethyl-3-cyclohexenyl)ethanal (**11**) and (1′*S*)-2-(4,6,6-trimethyl-3-cyclohexenyl)ethanal (**12**).

(1′*S*)-2-(2,2,4-Trimethyl-3-cyclohexenyl)ethanal (11). ^1H NMR (500 MHz, $CDCl_3$): δ 9.79 (dd, $J = 3.3$, 1.3 Hz, H−C(1)), 5.09 (dqd, $J = 2.2$, 1.4, 1.3 Hz, H−C(3′)), 2.54 (ddd, $J = 16.1$, 3.3, 1.3 Hz, H_a−C(2)), 2.15 (ddd, $J = 16.1$, 10.3, 3.3 Hz, H_b−C(2)), 1.98 (m, 1 H), 1.91 (m, 1 H), 1.85 (m, 1 H), 1.62 (m, 1 H), 1.61 (m, $H_3C(4'^1)$), 1.40 (m, 1 H), 0.99 (s, $H_3C_{eq}(2'^1)$), 0.82 (s, $H_3C_{ax}(2'^1)$). ^{13}C NMR (126 MHz, $CDCl_3$): δ 203.2 (d, C(1)), 132.3 (d, C(3′)), 131.3 (s, C(4′)), 45.2 (t, C(2)), 38.0 (d, C(1′)), 34.2 (s, C(2′)), 29.6 (t, C(5′)), 29.2 (q, $C_{eq}(2'^1)$), 25.3 (t, C(6′)), 23.7 (q, $C_{ax}(2'^1)$), 23.4 (q, $C(4'^1)$).

(1′*S*)-2-(4,6,6-Trimethyl-3-cyclohexenyl)ethanal (12). ^1H NMR (500 MHz, $CDCl_3$): δ 9.76 (dd, $J = 3.1$, 1.5 Hz, H−C(1)), 5.27 (m, H−C(3′)), 2.55 (dm, $J = 16.1$ Hz, H_a−C(2)), 2.14 (m, H−C(2′)), 2.13 (ddd, $J = 16.1$, 9.6, 3.1 Hz, H_b−C(2)), 1.95 (m, 1 H), 1.85 (m, 1 H), 1.72 (m, 1 H), 1.65 (m, 1 H), 1.61 (m, $H_3C(4'^1)$), 0.93 (s, $H_3C_{eq}(6'^1)$), 0.81 (s, $H_3C_{ax}(6'^1)$). ^{13}C NMR (126 MHz, $CDCl_3$): δ 203.2 (d, C(1)), 132.9 (s, C(4′)), 118.5 (d, C(3′)), 45.0 (t, C(2)), 44.6 (t, C(5′)), 36.6 (d, C(1′)), 31.6 (s, C(6′)), 29.5 (t, C(2′)), 28.6 (q, $C_{eq}(6'^1)$), 23.6 (q, $C(4'^1)$), 22.2 (q, $C_{ax}(6'^1)$).

Reductive Decomplexation of (−)-5. A solution of (−)-**5** (279 mg, 0.59 mmol) in degassed glacial acetic acid (20 mL) was irradiated at room temperature with a high-pressure mercury lamp (Pyrex filter) for 4 h. The resulting orange solution was extracted with pentane (3 × 20 mL), and the combined extracts were washed with water, dried over $MgSO_4$, and concentrated by distillation at atmospheric pressure. Chromatography on silica gel (*n*-pentane, $R_f = 0.65$) yields an inseparable mixture of two hydrocarbons (70 mg, 85% yield) in a 7:2 ratio according to capillary GC, identified by NMR as (4*R*)-1,4,5,5-tetramethylcyclohexene (**14**) and (4*R*)-1,3,3,4-tetramethylcyclohexene (**13**).

(4*R*)-1,3,3,4-Tetramethylcyclohexene (13). ^1H NMR (500 MHz, $CDCl_3$): δ 5.08 (ddq, $J = 2.2$, 1.4, 1.3 Hz, H−C(2)), 1.93 (dddddq, $J = 16.4$, 10.3, 6.1, 2.2, 1.1, 1.1 Hz, H_a−C(6)), 1.83 (*d*m, $J = 16.4$ Hz, H_b−C(6)), 1.61 (ddd, $J = 1.3$, 1.1, 0.9 Hz, $H_3C(1^1)$), 1.51 (ddd, $J = 10.2$, 6.1, 2.8 Hz, H_a−C(5)), 1.38 (m, 2 H, H−C(4), H_b−C(5)), 0.94 (s, $H_3C_{eq}(3^1)$), 0.86 (d, $J = 6.4$ Hz, $H_3C(4^1)$), 0.78 (s, $H_3C_{ax}(3^1)$). ^{13}C NMR (126 MHz, $CDCl_3$): δ 133.2 (d, C(2)), 130.9 (s, C(1)), 38.0 (d, C(4)), 32.2 (s, C(3)), 30.1 (t, C(6)), 29.4 (q, $C_{eq}(3^1)$), 27.9 (t, C(5)), 23.5 (q, $C(1^1)$), 22.9 (q, $C_{ax}(3^1)$), 16.0 (q, $C(4^1)$).

(4*R*)-1,4,5,5-Tetramethylcyclohexene (14). ^1H NMR (500 MHz, $CDCl_3$): δ 5.28 (m, H−C(2)), 2.00 (dm, $J = 17.3$ Hz, H_a−C(3)), 1.79 (dm, $J = 17.1$ Hz, H_a−C(6)), 1.67 (m, H_b−C(6)), 1.62 (m, $H_3C(1^1)$), 1.61 (dm, $J = 17.1$ Hz, H_b−C(3)), 1.41 (dqd, $J = 9.1$ Hz, 6.9 Hz, 5.4 Hz, H−C(4)), 0.90 (s, $H_3C_{eq}(5^1)$), 0.83 (d, $J = 6.9$ Hz, $H_3C(4^1)$), 0.75 (s, $H_3C_{ax}(5^1)$). ^{13}C NMR (126 MHz, $CDCl_3$): δ 132.7 (s, C(1)), 119.7 (d, C(2)), 45.4 (t, C(6)), 36.8 (d, C(4)), 32.2 (t, C(3)), 31.9 (s, C(5)), 28.9 (q, $C_{eq}(5^1)$), 23.7 (q, $C(1^1)$), 20.8 (q, $C_{ax}(5^1)$), 15.5 (q, $C(4^1)$).

X-ray Analysis. Crystallographic data and refinement details for compounds (+)-**2**, **3**, and (−)-**5** are given in Table 2. Intensity data were measured on a Stoe AED2 four-circle diffractometer, using graphite-monochromated Mo Kα radiation ($\lambda = 0.710\ 73$ Å). Compound (+)-**2** was measured in a Lindemann glass capillary at room temperature, while compounds **3** and (−)-**5** were measured in air at 193 K. Unit cell parameters were determined by least squares from the $\pm\omega$ values of 23, 20, and 21 reflections, respectively, in the range $14° < \theta < 17.5°$. For each compound three standard reflections were measured every 1 h and showed an intensity variation of 8% for (+)-**2**, 1.2% for **3**, and 0% for (−)-**5**. No corrections for absorption were made. The crystal structures were solved by direct methods and Fourier syntheses using the program SHELXS-86[20] and refined by the full-matrix least-squares method on F^2, using the program SHELXL-93.[21] Hydrogen atoms were included in calculated positions and treated as riding atoms using SHELXL-93 default parameters. Complex neutral atom scattering factors were taken from ref 22. Final positional and equivalent isotropic displacement parameters are given in the Supporting Information. Selected bond

(21) Sheldrick, G. M. SHELXS-93, Program for Crystal Structure Refinement; University of Göttingen, Göttingen, Germany, 1993.

(22) *International Tables for X-ray Crystallography*; D. Reidel: Dordrecht, The Netherlands, 1994; Vol. C.

distances and angles are given in Tables 3−5 and in the Supporting Information. The crystallographic numbering schemes are apparent from Figures 1−3, drawn using the program Platon.[23] Comparison of the Bijvoet pairs of complex (+)-**2** confirmed the absolute configuration deduced from the assumed ring-opening complexation mechanism involving pinene and pinene derivatives of known absolute configuration.

Acknowledgment. F. Fehr and F. Nydegger are thanked for measuring the NMR and mass spectra. The CIBA-GEIGY Co. is thanked for carrying out the elemental analyses. This work was supported by the Swiss National Science Foundation (Grant Nos. 20-31147.91, 20-37602.93, and 20-43347.95), which is gratefully acknowledged. H.S.-E. wishes to thank the Swiss National Science Foundation for an equipment grant (No. 2.372-0.84).

(23) Spek, A. L. PLATON. *Acta Crystallogr.* **1990**, *A46*, C34.

Supporting Information Available: Tables giving selected bond lengths and angles, atomic coordinates, and thermal parameters for (+)-**2**, **3**, and (−)-**5**. This material is available free of charge via the Internet at http://pubs.acs.org.

OM010781S